METALLOCENE POLYETHYLENE WAX SYNTHESIS

Jessica V. Lamb,† Jean-Charles Buffet,† Zoë R. Turner,† Tossapol Khamnaen,‡ and Dermot O′Hare(*)†

† Chemistry Research Laboratory, Department of Chemistry, University of Oxford, 12 Mansfield Road, Oxford, OX1 3TA, United Kingdom

‡ SCG Chemicals Co., Ltd, 1 Siam Cement Rd, Bangkok 10800, Thailand

Ethylene/H_2 polymerization, polyethylene wax, solid polymethylaluminoxane, high-throughput polymerization, permethylindenyl, zirconocenes

TOC

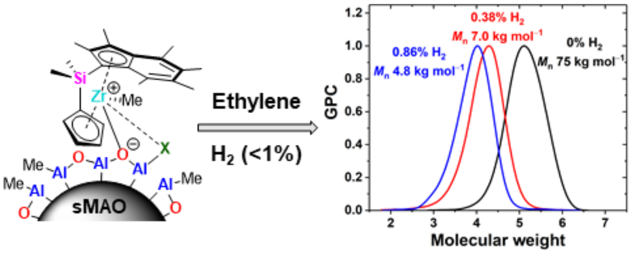

ABSTRACT

Solid polymethylaluminoxane (sMAO) supported *ansa*-bridged permethylindenyl zirconocenes $^{Me_2}SB(Cp^R,I^*)ZrX_2$ ($\{(\eta^5\text{-}C_9Me_6)Me_2Si(\eta^5\text{-}C_5H_3R)\}ZrX_2$; R = H, Me, and ^{n}Bu; X = Cl, Br, Me, and CH_2Ph) have been investigated as catalysts for the slurry-phase polymerization of ethylene in the presence of H_2. The catalysts demonstrated remarkable stability to H_2 both in a high-throughput screening system and in a 2 L batch reactor, with an almost constant ethylene uptake maintained throughout the polymerization runs. The catalysts demonstrated very high ethylene polymerization activities, almost three times higher than sMAO-$(Cp^{nBu})_2ZrCl_2$ (industrial standard zirconocene catalyst) under the same conditions. The presence of small quantities of H_2 (<1%) led to significant decreases in polymer molecular weights to produce commercially desirable polyethylene waxes (M_n <10 kg mol^{-1}) in the batch reactor.

INTRODUCTION

Polymer properties such as molecular weights (M_w and M_n), molecular weights distributions (MWD, M_w/M_n), the degree of branching, comonomer incorporation, and stereochemistry determine the potential applications of a polymer.[1] Dihydrogen (H_2) is a highly efficient chain transfer agent for the polymerization of α-olefins by metallocene catalysts and is often employed to both decrease and control polymer molecular weights.[2, 3] Contrary to conventional Ziegler–Natta catalysts, only a small quantity of H_2 is required to significantly reduce polymer molecular weights.[2, 4, 5]

Group 4 metallocenes are d^0 organometallic compounds containing two η^5-cyclopentadienyl (C_5H_5, Cp) ligands and two σ-type ligands (Cp_2MX_2). In comparison to traditional Ziegler–Natta catalysts,[6] metallocene catalysts provide a multitude of possibilities for synthesizing and controlling the structure and properties of polymers.[7-9] In addition, the single-site nature of metallocene catalysts usually results in polymers with unimodal molecular weight distributions.[10] Variation of the ancillary cyclopentadienyl ligands of Cp_2MX_2 species can influence polymerization activity and polymer properties. We recently reported a new family of unsymmetrical *ansa*-bridged zirconocenes based on the permethylindenyl ligand ($C_9Me_7^-$, Ind*, I*) as catalysts for ethylene and lactide polymerization (Chart 1).[11-15] When immobilized on solid polymethylaluminoxane (sMAO), an insoluble form of oligomeric methylaluminoxane (MAO), the species showed slurry-phase ethylene polymerization activities up to 9509 $kg_{PE}\ mol_{Zr}^{-1}\ h^{-1}\ bar^{-1}$; 34% more active than an industry-standard metallocene under the same conditions.[11] These systems produced polyethylenes with low molecular weights (M_n = 14 kg mol^{-1} for sMAO supported $^{Me_2}SB(Cp,I^*)ZrMe_2$ at 90 °C), and uniform, mono-disperse 'popcorn' morphologies.

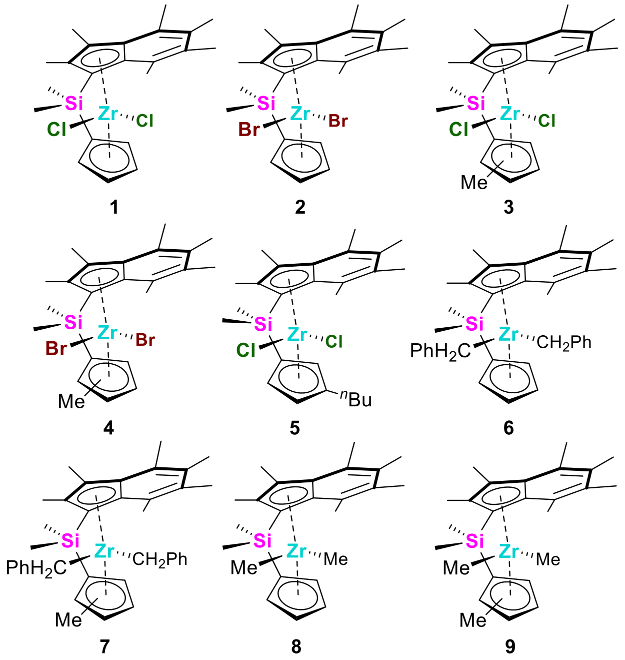

Chart 1. Group 4 permethylindenyl complexes $^{\mathrm{Me_2}}$SB(Cp,I*)ZrCl$_2$ (**1**),[12] $^{\mathrm{Me_2}}$SB(Cp,I*)ZrBr$_2$ (**2**),[11] $^{\mathrm{Me_2}}$SB(Cp$^{\mathrm{Me}}$,I*)ZrCl$_2$ (**3**),[12] $^{\mathrm{Me_2}}$SB(Cp$^{\mathrm{Me}}$,I*)ZrBr$_2$ (**4**),[11] *Z*-$^{\mathrm{Me_2}}$SB(Cp$^{n\mathrm{Bu}}$,I*)ZrCl$_2$ (**5**),[11] $^{\mathrm{Me_2}}$SB(Cp,I*)Zr(CH$_2$Ph)$_2$ (**6**),[11] $^{\mathrm{Me_2}}$SB(Cp$^{\mathrm{Me}}$,I*)Zr(CH$_2$Ph)$_2$ (**7**),[11] $^{\mathrm{Me_2}}$SB(Cp,I*)ZrMe$_2$ (**8**),[11] and $^{\mathrm{Me_2}}$SB(Cp$^{\mathrm{Me}}$,I*)ZrMe$_2$ (**9**).[11]

Polyethylene waxes (PE-waxes) are polymers with molecular weights (M_n) less than 10 kg mol^{-1}.[16, 17] PE-waxes can be made directly from the polymerization of ethylene under controlled conditions or by the thermal degradation of higher molecular weight polymers.[18, 19] Due to their hydrophobicity and chemical and heat stability,[20, 21] PE-waxes are used in plastic processing applications to improve product physical appearance and thermal properties. PE-waxes are also commonly used as additives to impart mark, slip, rub, and scratch resistance in printing inks and paints, improve the fusing properties in toner formulations, improve the mechanical properties of surface coatings, and act as lubricating agents in plastic processing.[18, 19, 22-24] PE-wax dispersions, obtained by the redispersion of low-density polyethylene (LDPE) in water,[24-26] are targeted for use in coating applications in the paper industry.[27] They are also used as surface modifiers for primers, paints, inks, coatings, and lubricants.[24] Additionally, PE-wax emulsions, prepared by mixing modified high-density polyethylene (HDPE) with an emulsifier and water, have shown applications in packaging.[28]

Limited examples of group 4 metallocenes have been reported as catalysts for the production of polyethylene waxes.[17, 29, 30] However, there is a great incentive for their use as traditional Ziegler–Natta catalysts usually result in significant reactor fouling due to the broad molecular weight distributions of the waxes produced, which also contain substantial amounts of undesirable ethylene oligomers.[30] Napoli *et al.* reported that when group 4 metallocenes such as bis(cyclopentadienyl)zirconium dichloride (Cp_2ZrCl_2), *rac*-ethylenebis(1-indenyl)zirconium dichloride (*rac*-(EBI)$ZrCl_2$) and *rac*-dimethylsilyl-bis(2-methyl-4-phenyl-1-indenyl)zirconium dichloride (*rac*-^{Me_2}SB($^{2\text{-Me,4-Ph}}$Ind)$ZrCl_2$) were activated by MAO, they polymerized ethylene in the solution phase in the presence of H_2 and produced polyethylene waxes with molecular weights (M_n) less than 12 kg mol^{-1} and narrow molecular weight distributions (M_w/M_n = 2.0–3.5).[17] In the patent literature, catalysts comprising of a group 4 metallocenes, such as bis(cyclopentadienyl)dimethyl zirconium (Cp_2ZrMe_2) and Cp_2ZrCl_2, with an aluminoxane activator have been shown to produce polyethylene waxes with molecular weights (M_w) of 2–10 kg mol^{-1} and varying molecular weight distributions (M_w/M_n = 2–10) at relatively low temperatures (70–90 °C) with H_2 partial pressures of 1–10%.[29] Group 4 metallocenes such as bis(*n*-butylcyclopentadienyl)zirconium dichloride ($(Cp^{n\text{Bu}})_2ZrCl_2$) activated with trimethylaluminum (TMA) and immobilized onto an aluminoxane coated silica gel have also been shown to produce polyethylene waxes with narrow molecular weight distributions ($M_w/M_n \leq 5$) from the gas phase polymerization of ethylene in the presence of high amounts of H_2 (7 mol%).[30]

High-throughput screening is a useful tool for simultaneously testing catalysts under a variety of different conditions via robotic systems that automate sample preparation, handling, and data analysis.[31, 32] Miniaturized, automated, parallel reaction set-ups have been implemented for the rapid assessment of novel catalyst applications, while also being used for the generation of reliable kinetic data for mechanistic studies.[33, 34] High-throughput screening allows for reduced time in the design of new materials and faster optimization of reaction conditions.[35] It also offers multiple technical, economic and environmental advantages over conventional processes; the small size of the reactors leads to decreased costs, chemical consumption and waste, in addition to the increased probability of discovering materials or conditions with the desired properties or results in a shorter time period.[33] Busico and co-workers demonstrated that for a $MgCl_2/TiCl_4$-$AlEt_3$ Ziegler-Natta catalyst, a high-throughput system gave the same ethylene/1-hexene co-polymerization results as a 2 L batch reactor for catalyst activity, polymer molecular weights, and 1-hexene incorporation.[33]

High-throughput screening has also been shown to be a useful technique for the identification of new, selective organometallic catalysts for olefin polymerization.[32, 33, 36, 37] For example, the development of pyridyl-amide hafnium catalysts for the homopolymerization of 1-alkenes to produce highly isotactic polymers.[36, 38] The initial target was to identify novel catalysts for ethylene/1-octene copolymerization; however, high-throughput screening resulted in the identification of a catalyst with the ability to homopolymerize 1-alkenes isoselectively.

Herein, we report the synthesis of polyethylene waxes with narrow molecular weight distributions using highly active supported permethylindenyl zirconocene catalysts in a high-throughput screening system and large-scale batch reactor.

RESULTS AND DISCUSSION

High-throughput ethylene/H_2 polymerization The complexes in Chart 1 were immobilized on solid polymethylaluminoxane (sMAO) with an initial aluminum to zirconium catalyst loading ($[Al_{sMAO}]_0/[Zr]_0$) of 200.[11] Polymerizations were conducted in a high-throughput system, which allowed for multiple catalysts and conditions to be tested simultaneously in miniaturized, automated, parallel reaction set-ups.[31, 32] High-throughput polymerization studies were conducted in a parallel pressure reactor (PPR) in 23 mL cells with 5 mL heptane, 10 µmol triisobutylaluminum (TiBA, $Al(CH_2CH(CH_3)_2)_3$) scavenger, 0.05–0.15 mg pre-catalyst, 8.3 bar ethylene, and 0.8% (0.07 bar) or 1.6% (0.13 bar) H_2 supplied by a mixed H_2/N_2 feed. Reactions were run at 80 °C for 1 hour or until 8.3 bar ethylene uptake was reached. sMAO supported $^{Me_2}SB(Cp,I^*)ZrCl_2$ ($\mathbf{1}_{\mathbf{sMAO}}$), $^{Me_2}SB(Cp,I^*)ZrBr_2$ ($\mathbf{2}_{\mathbf{sMAO}}$), $^{Me_2}SB(Cp^{Me},I^*)ZrCl_2$ ($\mathbf{3}_{\mathbf{sMAO}}$), $^{Me_2}SB(Cp^{Me},I^*)ZrBr_2$

(**4**$_{\mathbf{sMAO}}$), *Z*-$^{\mathrm{Me_2}}$SB(Cp$^{n\mathrm{Bu}}$,I*)ZrCl$_2$ (**5**$_{\mathbf{sMAO}}$), $^{\mathrm{Me_2}}$SB(Cp,I*)Zr(CH$_2$Ph)$_2$ (**6**$_{\mathbf{sMAO}}$), $^{\mathrm{Me_2}}$SB(Cp$^{\mathrm{Me}}$,I*)Zr(CH$_2$Ph)$_2$ (**7**$_{\mathbf{sMAO}}$), $^{\mathrm{Me_2}}$SB(Cp,I*)ZrMe$_2$ (**8**$_{\mathbf{sMAO}}$), and $^{\mathrm{Me_2}}$SB(Cp$^{\mathrm{Me}}$,I*)ZrMe$_2$ (**9**$_{\mathbf{sMAO}}$) were studied.

For catalysts of this type, H_2 is anticipated to cause a reduction in ethylene uptake rate over time. However, the ideal targets are systems that are not deactivated by H_2 and maintain constant ethylene uptake rates throughout the polymerization runs. The in-situ ethylene uptake rate profiles of **1**$_{\mathbf{sMAO}}$–**9**$_{\mathbf{sMAO}}$ highlight the stability of these catalysts in the presence of H_2 (Figures 1 and S1–S4). When H_2 was present, the ethylene uptake rates were lower than polymerization without H_2; uptake rates of 11.77, 4.82, and 3.58 psi min^{-1} for **8**$_{\mathbf{sMAO}}$ with 0, 0.8, and 1.6% H_2 respectively after 600 seconds (Figure 1). The uptake rates were also observed to slowly decrease over time (from 4.69 psi min^{-1} after 200 seconds to 2.98 psi min^{-1} after 1800 seconds for **6**$_{\mathbf{sMAO}}$, Figure S3a). However, all the catalysts maintained significant ethylene uptake rates on completion of the polymerization runs. **8**$_{\mathbf{sMAO}}$ showed the highest stability to H_2, with a constant ethylene uptake rate of approximately 3.50 psi min^{-1} throughout the polymerization with 1.6% H_2 (Figure 1).

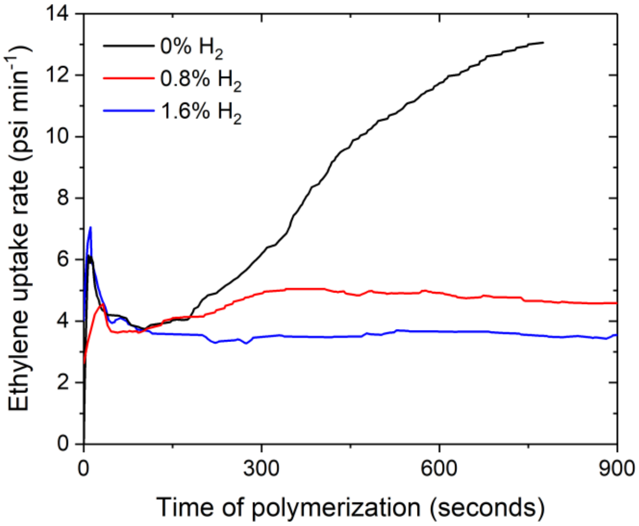

Figure 1. Slurry-phase polymerization ethylene uptake rate as a function of time of polymerization using sMAO supported $^{\mathrm{Me_2}}$SB(Cp,I*)ZrMe$_2$ (**8**$_{\mathbf{sMAO}}$) with 0 (black), 0.8 (red), and 1.6% H_2 (blue). Polymerization conditions: $[\mathrm{Al_{sMAO}}]_0/[\mathrm{Zr}]_0 = 200$, TiBA (10 µmol), ethylene (8.3 bar), pre-catalyst (0.05 mg), heptane (5 mL), and 80 °C. Reactions quenched at 8.3 bar ethylene uptake or after 1 hour.

The catalysts showed a significant decrease in ethylene polymerization activity when H_2 was introduced to the system (Figures 2 and S7; Table 1); however, they remained very active with activities of 44000, 18000, and 16000 $\mathrm{kg_{PE}\ mol_{Zr}^{-1}\ h^{-1}\ bar^{-1}}$ for **1**$_{\mathbf{sMAO}}$ with 0, 0.8, and 1.6% H_2 respectively. The presence of H_2 offers an alternative termination pathway to those typically observed for ethylene polymerization (such as transfer to another ethylene monomer, β-hydride elimination, and chain transfer to the aluminum co-catalyst)[39-41] whereby H_2 binds to the free coordination site of the catalyst, leading to the release of the polymer chain and formation of a metal hydride species.[40] The reduction in polymerization rate in the presence of H_2 can be rationalized due to an increase in the formation of the metal hydride termination product, which requires reactivation for propagation by insertion of a monomer unit.[40, 42] It has been found that the rate of insertion of ethylene into the Zr–H bond of the metal hydride is significantly slower than the rate of insertion into the Zr–Me bond of the catalyst, leading to a reduction in polymerization rate.[43-46] This has been modeled for the polymerization of 1-hexene using (EBI)$ZrMe_2/B(C_6F_5)_3$, where the rate of reinitiation of Zr–H was found to be more than 1 order of magnitude slower than the rate of propagation of Zr–Me.[47] Solution phase ethylene/H_2 polymerization data using *rac*-^{Me_2}SB$^{(2\text{-}Me,4\text{-}Ph}$Ind)$ZrCl_2$ activated with MAO have shown that the activity increased from 770 to 1185 $\mathrm{kg_{PE}\ mol_{Zr}^{-1}\ h^{-1}\ bar^{-1}}$ for ethylene/H_2 polymerization (4.5 bar ethylene, 1.5 bar H_2, and 80 °C).[17] However, the deactivating effect of H_2 has been demonstrated for homogeneous ethylene polymerization using Cp_2ZrCl_2/MAO, where activity decreased from 45000 to 21400 $\mathrm{kg_{PE}\ mol_{Zr}^{-1}\ h^{-1}\ bar^{-1}}$ with 0 and 0.5 mol% H_2 respectively (8 bar ethylene and 70 °C).[5] After an initial increase in activity, Cp_2ZrCl_2 supported on MAO activated silica was also shown to experience a decrease in slurry-phase ethylene polymerization activity with increasing amounts of H_2; activities of 430 and 400 $\mathrm{kg_{PE}\ mol_{Zr}^{-1}\ h^{-1}\ bar^{-1}}$ with 0 and 4.1 bar H_2 respectively (5.5 bar ethylene and 60 °C).[50]

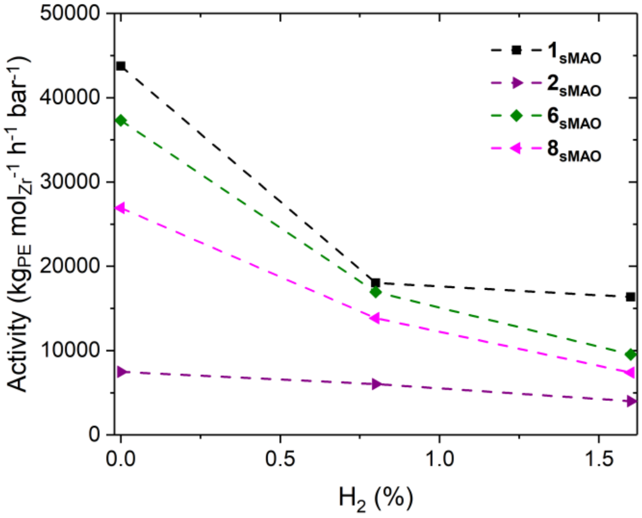

Figure 2. Slurry-phase ethylene polymerization activity as a function of H_2 (%) using sMAO supported ^{Me_2}SB(Cp,I*)$ZrCl_2$ (**1**$_{\mathbf{sMAO}}$) (black square), ^{Me_2}SB(Cp,I*)$ZrBr_2$ (**2**$_{\mathbf{sMAO}}$) (purple right triangle), ^{Me_2}SB(Cp,I*)$Zr(CH_2Ph)_2$ (**6**$_{\mathbf{sMAO}}$) (green diamond), and ^{Me_2}SB(Cp,I*)$ZrMe_2$ (**8**$_{\mathbf{sMAO}}$) (pink left triangle). Polymerization conditions: $[Al_{sMAO}]_0/[Zr]_0 = 200$, TiBA (10 μmol), ethylene (8.3 bar), pre-catalyst (0.05–0.15 mg), heptane (5 mL), and 80 °C. Reactions quenched at 8.3 bar ethylene uptake or after 1 hour.

For sMAO-^{Me_2}SB(Cp^R,I*)$ZrCl_2$ catalysts, activity follows the same trend observed in previous work for ethylene homopolymerization using 2 bar ethylene and 50 mL solvent;[11] R = H > Me > ^{n}Bu (**1**$_{\mathbf{sMAO}}$ > **3**$_{\mathbf{sMAO}}$ > **5**$_{\mathbf{sMAO}}$) (Table 1 and Figure S7b). This is rationalized due to larger R substituents obstructing the metal center and inhibiting the initial coordination of ethylene monomers. For sMAO-^{Me_2}SB(Cp,I*)ZrX_2 catalysts, activity follows the order X = Cl > CH_2Ph > Me > Br (**1**$_{\mathbf{sMAO}}$ > **6**$_{\mathbf{sMAO}}$ > **8**$_{\mathbf{sMAO}}$ > **2**$_{\mathbf{sMAO}}$), which was also observed in previous work (Figure 2 and Table 1).[11] As the same cationic species is usually formed regardless of the identity of the initiation group,[7, 51, 52] the differences in activity suggests that polymerization activity is at least partially dependent on the efficiency of initiation group abstraction by the co-catalyst and by the presence of the initiating group on the surface of the inorganic support. For sMAO-^{Me_2}SB(Cp^{Me},I*)ZrX_2 catalysts, X = Cl (**3**$_{\mathbf{sMAO}}$) displays a much higher polymerization activity than X = Me, CH_2Ph or Br in the presence of H_2, which is in contrast to sMAO-^{Me_2}SB(Cp,I*)ZrX_2 and previous studies and may be due to differences in the rate of formation of the metal hydride species (Table 1 and Figure S7a).

In general, gel permeation chromatography (GPC) showed the polymers produced in the presence of 1.6% H_2 had molecular weights (M_n) approximately 20 times smaller than in the systems without H_2; for example, M_n = 120 and 6.1 kg mol^{-1} for $\mathbf{8_{sMAO}}$ with 0 and 1.6% H_2 respectively (Figures 3 and S9–13; Table 1). M_n was also observed to decrease as more H_2 was added to the system; for example, M_n = 120, 14, and 6.9 kg mol^{-1} for $\mathbf{6_{sMAO}}$ with 0, 0.8, and 1.6% H_2 respectively.

Table 1. Slurry-phase ethylene/H_2 polymerization using sMAO supported complexes in a high-throughput system.[a]

Catalyst	**H_2 [b]**	**Activity [c]**	**M_n [d]**	**M_w/M_n**
$\mathbf{1_{sMAO}}$	0	44000	110	3.2
	0.8	18000	14	2.3
	1.6	16000	11	2.0
$\mathbf{2_{sMAO}}$	0	7500	120	2.4
	0.8	6000	11	2.6
	1.6	4000	7.1	2.6
$\mathbf{3_{sMAO}}$	0	20000	110	3.0
	0.8	16000	11	2.9
	1.6	12000	5.1	2.9
$\mathbf{4_{sMAO}}$	0	6600	120	2.9
	0.8	3500	8.9	3.4
	1.6	1900	4.5	3.6
$\mathbf{5_{sMAO}}$	0	38000	63	2.4
	0.8	4000	6.7	3.6
	1.6	3800	4.3	3.4
$\mathbf{6_{sMAO}}$	0	37000	120	2.5
	0.8	17000	14	2.5

	1.6	9500	6.9	2.4
7$_{\mathbf{sMAO}}$	0	23000	110	3.3
	0.8	5000	7.5	3.7
	1.6	4000	3.9	3.9
8$_{\mathbf{sMAO}}$	0	27000	120	3.0
	0.8	14000	11	2.6
	1.6	7400	6.1	2.7
9$_{\mathbf{sMAO}}$	0	17000	110	3.1
	0.8	3400	6.9	3.6
	1.6	2660	3.9	3.8

(a) Polymerization conditions: $[Al_{sMAO}]_0/[Zr]_0 = 200$, TiBA (10 μmol), ethylene (8.3 bar), pre-catalyst (0.05–0.15 mg), heptane (5 mL), and 80 °C. Reactions quenched at 8.5 bar ethylene uptake or after 1 hour; (b) %; (c) $kg_{PE}\ mol_{Zr}^{-1}\ h^{-1}\ bar^{-1}$, reported to 2 significant figures; (d) $kg\ mol^{-1}$, reported to 2 significant figures.

The polymers produced in the presence of H_2 are classed as ultra-low molecular weight polyethylenes, PE-wax, with M_n of 4–11 kg mol^{-1}. The decrease in molecular weights in the presence of H_2 is most likely due to the increased amount of chain termination that occurs when H_2 acts as a chain transfer agent. A decrease in polymer molecular weights in the presence of H_2 has also been observed by Soares and co-workers when using *rac*-(EBI)$ZrCl_2$ supported on MAO treated silica; M_w decreased from approximately 100 to 3 kg mol^{-1} in the presence of 2 bar H_2 (60 °C and 5.5 bar ethylene).[50]

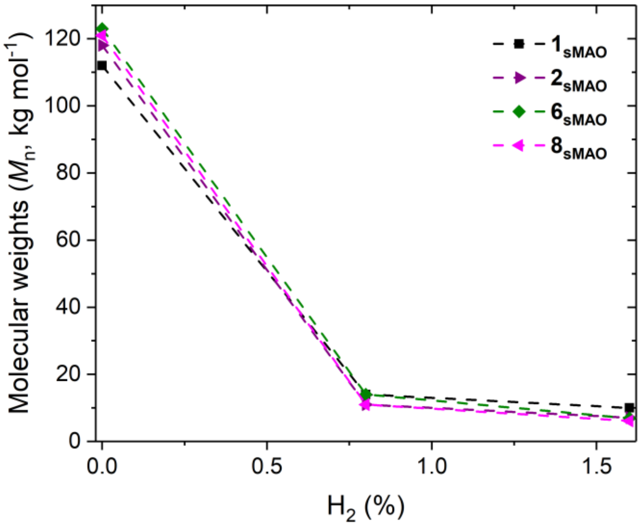

Figure 3. Polymer molecular weights (M_n) as a function of H_2 (%) for the polymers produced using sMAO supported $^{Me_2}SB(Cp,I^*)ZrCl_2$ ($\mathbf{1_{sMAO}}$) (black square), $^{Me_2}SB(Cp,I^*)ZrBr_2$ ($\mathbf{2_{sMAO}}$) (purple right triangle), $^{Me_2}SB(Cp,I^*)Zr(CH_2Ph)_2$ ($\mathbf{6_{sMAO}}$) (green diamond), and $^{Me_2}SB(Cp,I^*)ZrMe_2$ ($\mathbf{8_{sMAO}}$) (pink left triangle). Polymerization conditions: $[Al_{sMAO}]_0/[Zr]_0 = 200$, TiBA (10 µmol), ethylene (8.3 bar), pre-catalyst (0.05–0.15 mg), heptane (5 mL), and 80 °C. Reactions quenched at 8.3 bar ethylene uptake or after 1 hour.

The activation barrier for H_2 insertion has been calculated to be lower than that for ethylene insertion, indicating why only a small amount of H_2 is required to reduce polymer molecular weights drastically.[53] The molecular weight distributions (M_w/M_n) were found to be fairly narrow and unaffected by the presence of H_2, ranging between 2.0 to 3.9 for all solid MAO supported catalysts, indicating that these species behave largely as single-site catalysts (Table 1).

Crystallization-elution fractionation (CEF) was used to measure the elution temperature ($T_{el,max}$) of the polymers, which decreases as the melting point and crystallinity of the polymer decreases. $T_{el,max}$ was found to decrease slightly in the presence of H_2 ($T_{el,max}$ of 110.9, 109.9, and 109.3 °C with 0, 0.8, and 1.6% H_2 respectively for $\mathbf{8_{sMAO}}$), indicating that melting point and crystallinity also decrease slightly in the presence of H_2 (Table S1; Figures S18 and S19). The amorphous fraction (AF) increased as the H_2 concentration increased; AF ≤0.4, ≤2.2, and ≤3.5 wt% for all catalysts with 0, 0.8, and 1.6% H_2 respectively.

Large scale ethylene/H_2 polymerization **1_{sMAO}, $3s_{MAO}$, 6_{sMAO}, 7_{sMAO}** and **8_{sMAO}** were studied for ethylene/H_2 polymerization in 2 L steel batch reactors. Polymerizations were run at 80 °C for 1 hour with 1 L hexane, 2.5 mL triethylaluminum (TEA, $Al_2(C_2H_5)_6$) scavenger, 0.025–0.070 g pre-catalyst, $[Al_{sMAO}]_0/[Zr]_0$ of 200, 8 bar ethylene gas, and either 0, 0.38 (0.03 bar) or 0.86% (0.07 bar) H_2.

Similar to the high-throughput system, the presence of H_2 decreased the ethylene uptake rate compared to polymerization without H_2; uptake rates of 17.81 and 5.28 L mg_{CAT}^{-1} min^{-1} for **8_{sMAO}** after 60 minutes with 0 and 0.86% H_2 respectively (Figures 4, S5, and S6).

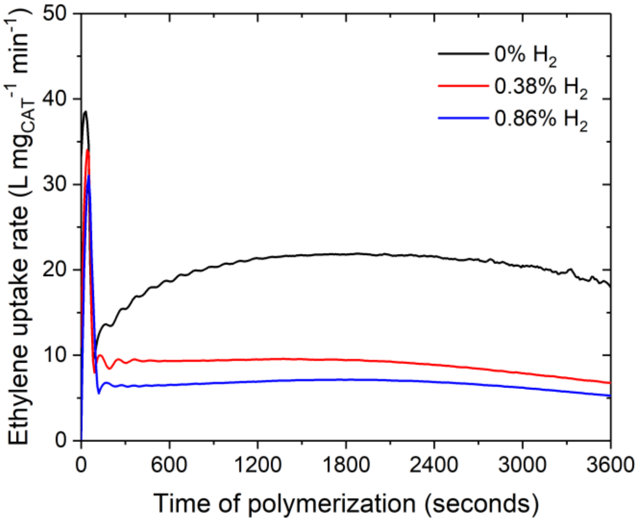

Figure 4. Slurry-phase polymerization ethylene uptake rate as a function of time of polymerization using sMAO supported $^{Me_2}SB(Cp,I^*)ZrMe_2$ (**8_{sMAO}**) with 0 (black), 0.38 (red), and 0.86% H_2 (blue). Polymerization conditions: $[Al_{sMAO}]_0/[Zr]_0 = 200$, TEA (0.5 mmol), ethylene (8 bar), pre-catalyst (0.025–0.050 g), hexane (1 L), 80 °C, and 1 hour.

For most catalysts, the uptake rate was also shown to decrease gradually over time; for example, 5.76 and 3.08 L mg_{CAT}^{-1} min^{-1} for **6_{sMAO}** after 600 and 3600 seconds respectively with 0.86% H_2. However, **1_{sMAO}** and **8_{sMAO}** displayed the highest stability to H_2, with uptake rates of 6.54 and 5.28 L mg_{CAT}^{-1} min^{-1} for **8_{sMAO}** after 600 and 3600 seconds respectively with 0.86% H_2.

As observed in the high-throughput system, activity decreased as the amount of H_2 in the reactor was increased. However, all catalysts maintain very high activities (Table 2 and Figure S8). For **1_{sMAO}** and

$\mathbf{8_{sMAO}}$, activity decreased by approximately half and one third respectively with 0 and 0.86% H_2; from 30000 to 13000 $kg_{PE}\,mol_{Zr}^{-1}\,h^{-1}\,bar^{-1}$ and from 27000 to 8900 $kg_{PE}\,mol_{Zr}^{-1}\,h^{-1}\,bar^{-1}$ respectively. In addition to the formation of the metal hydride species, the reduction in activity on the introduction of H_2 to the system may be due to the decreased solubility of ethylene monomers in the hexane solvent in the presence of H_2.[54] For $\mathbf{1_{sMAO}}$, additional experiments were run using higher concentrations of H_2 (2.00 and 3.50%). When H_2 was increased from 0.86% to 3.50%, activity decreased by approximately a third to 4200 $kg_{PE}\,mol_{Zr}^{-1}\,h^{-1}\,bar^{-1}$. When compared to an industrial standard, sMAO supported $(Cp^{nBu})_2ZrCl_2$, $\mathbf{1_{sMAO}}$ afforded productivities almost three times higher under the same polymerization conditions; productivities of 1.2 and 3.2 $kg_{PE}\,g_{CAT}^{-1}$ respectively with 3.50% H_2.

Polymer molecular weights (M_n) significantly decreased with increasing H_2 concentration; from 75 to 4.8 kg mol^{-1} for $\mathbf{8_{sMAO}}$ with 0 and 0.86% H_2 respectively (Table 2 and Figures S14–S17). For $\mathbf{1_{sMAO}}$, the molecular weights of the isolated polymers continued to decrease as the amount of H_2 in the system was increased further. The lowest recorded polymer molecular weights were isolated using $\mathbf{1_{sMAO}}$ in the presence of 2.00 and 3.50% H_2, with M_n reaching as low as 1.7 kg mol^{-1}. This demonstrates the applications of these catalysts for the production of commercially viable polyethylene waxes. In general, the molecular weight distributions of the polymers were unaffected by the presence of H_2 (Table 2). However, M_w/M_n was observed to increase when moving from the high-throughput system to the batch reactor, especially for $\mathbf{1_{sMAO}}$; M_w/M_n of 3.2 and 5.0 with 0% H_2 in the high-throughput and batch reactor respectively. This may be due to the different conditions of polymerization between the two systems (e.g. TiBA vs. TEA activator, heptane vs. hexane solvent or variations in how the ethylene and H_2 are supplied to the reactor) and indicates that polymerization is less controlled on a larger scale.

Table 2. Slurry-phase ethylene/H_2 polymerization using sMAO supported complexes in a 2 L batch reactor.[a]

Catalyst	**H_2 [b]**	**Activity [c]**	**M_n [d]**	**M_w/M_n**

$\mathbf{1_{sMAO}}$	0	30000	53	5.0
	0.86	13000	-	-
	2.00	6400	2.1	5.8
	3.50	4200	1.7	6.5
$\mathbf{3_{sMAO}}$	0	12000	69	3.6
	0.38	7400	9.7	3.5
	0.86	7600	5.0	3.8
$\mathbf{6_{sMAO}}$	0	12000	71	3.8
	0.38	6900	9.2	3.0
	0.86	6700	5.2	2.7
$\mathbf{7_{sMAO}}$	0	22000	69	3.0
	0.38	9500	6.8	4.1
	0.86	7200	4.6	4.1
$\mathbf{8_{sMAO}}$	0	27000	75	3.0
	0.38	12000	7.0	3.8
	0.86	8900	4.8	3.2

(a) Polymerization conditions: $[Al_{sMAO}]_0/[Zr]_0 = 200$, TEA (2.5 mL), ethylene (8 bar), pre-catalyst (0.025–0.070 g), hexane (1 L), 80 °C, and 1 hour; (b) %; (c) $kg_{PE}\ mol_{Zr}^{-1}\ h^{-1}\ bar^{-1}$, reported to 2 significant figures; (d) $kg\ mol^{-1}$.

Scanning electron microscopy (SEM) shows that the polyethylenes formed in the absence of H_2 have very uniform, 'popcorn' morphologies (Figure S20).[11] The presence of H_2 was found to have little effect on the morphologies of the polymers, with the same 'popcorn' morphology observed using $\mathbf{1_{sMAO}}$ with 0, 2.00, and 3.50% H_2 (Figures 5, S20, and S21).

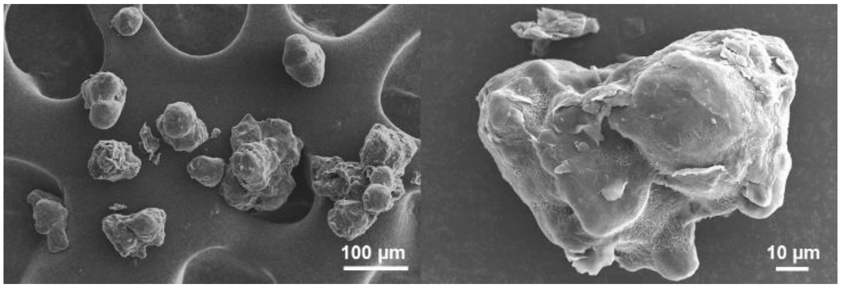

Figure 5. SEM images at ×200 and ×1000 magnification of the polymers produced from the slurry-phase polymerization of ethylene using $\mathbf{1}_{\mathbf{sMAO}}$ in the presence of 2.00% H_2.

The polymers produced using $\mathbf{7}_{\mathbf{sMAO}}$ and $\mathbf{8}_{\mathbf{sMAO}}$ were found by differential scanning calorimetry (DSC) to have a high crystallinity (83 and 86% respectively in the presence of 0.86% H_2) and melting temperature (T_m) indicative of high-density polyethylene (HDPE) with minimal defects and branching; 130 °C in the presence of 0.86% H_2. Density measurements further confirmed the production of HDPE (0.98 g cm^{-3}).

High-throughput ethylene/H_2/1-hexene copolymerization Due to a phenomenon known as the comonomer effect, metallocene catalysts can experience an increase in ethylene polymerization activity on the introduction of long-chain α-olefins, such as 1-hexene.[3, 55-57] The origin of this effect is unclear; however, it is most widely accepted that α-olefin incorporation decreases polymer crystallinity, which leads to an increase in polymer solubility in the reaction medium. This causes the catalytic sites to become more accessible and allows for more facile monomer diffusion.[58-60] Additionally, molecular simulations also show that ethylene solubility is enhanced by up to 10% on the addition of 5 mol% 1-hexene at 70–100 °C, which could then lead to an increase in activity.[61] However, the comonomer effect cannot always be explained as a purely physical phenomenon, and changes in the chemistry of the active sites must be considered.[62] One possible explanation is a 'trigger mechanism' whereby the active sites of the catalyst coordinate two monomers (in addition to the polymer chain),[63] with coordination of the second monomer 'triggering' insertion of the first.[64] This has been expanded to propose that when two different monomers are present (e.g. ethylene and a more electron-rich α-olefin) then the α-olefin stabilizes the active site and 'triggers' insertion of ethylene, leading to an enhancement in activity.[62, 65]

For these catalyst systems, it was postulated that combining the increase in ethylene uptake rate usually observed for ethylene/1-hexene copolymerizations may reduce some of the deactivating effects of H_2. The incorporation of longer chain α-olefin monomers into polyethylene chains can also increase the degree of polymer branching, and therefore lower the melting point, crystallinity, and density.[66] This increases the flexibility of the polymer and allows applications in packaging, foams, elastic fibers, and adhesives.[67]

Slurry-phase ethylene/H_2/1-hexene copolymerization high-throughput studies were conducted at 80 °C for 1 hour or until 5.5 bar ethylene uptake was reached. Polymerizations were run using 5 mL heptane, 10 µmol TiBA scavenger, 0.05–0.10 mg pre-catalyst, 150 or 250 µL 1-hexene (2.5 or 5.0% of the total reaction volume), $[Al_{sMAO}]_0/[Zr]_0$ of 200, 8.3 bar ethylene, and 0.8% (0.07 bar) H_2 supplied by a mixed H_2/N_2 feed. sMAO supported $^{Me_2}SB(Cp^{Me},I^*)ZrBr_2$ ($\mathbf{4_{sMAO}}$), $^{Me_2}SB(Cp^{nBu},I^*)ZrCl_2$ ($\mathbf{5_{sMAO}}$), $^{Me_2}SB(Cp^{Me},I^*)Zr(CH_2Ph)_2$ ($\mathbf{7_{sMAO}}$), and $^{Me_2}SB(Cp^{Me},I^*)ZrMe_2$ ($\mathbf{9_{sMAO}}$) were studied.

The uptake rate profiles show an initial increase in ethylene uptake rate due to the comonomer effect, which begins to decrease after approximately 300 seconds (Figures S22 and S23). The catalysts experienced an increase in polymerization activity with 125 µL 1-hexene and 0.8% H_2 when compared to ethylene/H_2 homopolymerization due to the comonomer effect (Table 3 and S26). However, with 250 µL 1-hexene, all catalysts except $\mathbf{7_{sMAO}}$ experienced a decrease in polymerization activity compared to the ethylene/H_2 system with 125 µL 1-hexene. This decrease in activity could be due to competitive coordination between ethylene and 1-hexene monomers at the active metal center; upon coordination, if the rate of 1-hexene insertion is slower than ethylene insertion, the rate of ethylene uptake decreases and leads to a decrease in polymerization activity.[68] The decrease in activity may also be due to slower rates of monomer insertion; insertion into the branched alkyl active species [R–1-hexene–cat] that forms following 1-hexene insertion is typically slower than insertion into unbranched alkyl active species [R–ethylene–cat] due to the increased steric bulk of the α-olefin.[69]

Table 3. Slurry-phase ethylene/H_2/1-hexene copolymerization using sMAO supported complexes in a high-throughput system.[a]

Catalyst	1-Hexene [b]	Activity [c]	M_n [d]	M_w/M_n
$\mathbf{4}_{\mathbf{sMAO}}$	0	3500	8.9	3.4
	125	7900	11	2.8
	250	4500	14	2.7
$\mathbf{5}_{\mathbf{sMAO}}$	0	4100	6.7	3.6
	125	21000	10	2.5
	250	14000	12	2.4
$\mathbf{7}_{\mathbf{sMAO}}$	0	5000	7.5	3.7
	125	19000	8.0	3.0
	250	24000	11	2.8
$\mathbf{9}_{\mathbf{sMAO}}$	0	3400	6.9	3.6
	125	13000	9.2	2.8
	250	13000	11	2.8

(a) Polymerization conditions: 0.8% H_2, $[Al_{sMAO}]_0/[Zr]_0 = 200$, TiBA (10 µmol), ethylene (8.3 bar), pre-catalyst (0.05–0.10 mg), heptane (5 mL), and 80 °C; reactions quenched at 5.5 or 8.3 bar ethylene uptake for co- and homopolymerization respectively or after 1 hour; (b) µL; (c) $kg_{PE}\ mol_{Zr}^{-1}\ h^{-1}\ bar^{-1}$, reported to 2 significant figures; (d) $kg\ mol^{-1}$.

A decrease in activity for ethylene/1-hexene copolymerization has been observed in other zirconocene systems, such as for the solution-phase copolymerization of ethylene and 1-hexene using $(^{2\text{-Ph}}Ind)_2ZrCl_2$ with MAO co-catalyst where activity decreased from 2200 to 960 $kg_{PE}\ mol_{Zr}^{-1}\ h^{-1}\ bar^{-1}$ with 0 and 0.16 M 1-hexene respectively and 1 bar ethylene.[70] The deactivating effects of 1-hexene have also been observed in heterogeneous systems; the copolymerization of ethylene and 1-hexene using $(^{2,4\text{-Me}}Ind)_2ZrCl_2$ supported on silica with MAO co-catalyst showed a decrease in activity from 4640 to 200 $kg_{PE}\ mol_{Zr}^{-1}\ h^{-1}\ bar^{-1}$ with 0 and 0.8 M 1-hexene respectively and 1 bar ethylene.[71]

Molecular weights (M_n) were observed to increase slightly when 1-hexene was added to the system, suggesting that competitive monomer coordination between ethylene, H_2 and 1-hexene hindered termination processes; M_n of 6.9, 9.2 and 11 kg mol−1 for **9_{sMAO}** with 0.8% H_2 and 0, 125 and 250 μL 1-hexene respectively (Table 3; Figures S27–S29). This may be because the increase in chain propagation from the higher ethylene/1-hexene copolymerization activity is greater than the increase in chain termination caused by chain transfer to H_2. An increase in polymer molecular weights for ethylene/1-hexene copolymerization has been observed in solution-phase polymerization using 2,4-cyclopentadien-1-ylidene(isopropylidene)-fluoren-9-ylidene zirconium dichloride (^{Me_2}CB(Flu,Cp)$ZrCl_2$) with MAO co-catalyst.[72]

The percentage incorporation of 1-hexene in the polymer chain was determined by $^{13}C\{^1H\}$ NMR spectroscopy as 0.6–0.7 and 1.0–1.1 mol% for all catalysts with 125 and 250 μL 1-hexene respectively in the presence of 0.8% H_2 (Table S2). CEF showed that Tel,max. decreased as the proportion of 1-hexene in the polymer increased; $T_{el,max.}$ = 110.5, 105.7, and 103.2 °C for **5_{sMAO}** with 0.8% H_2 and 0, 125, and 250 μL 1-hexene respectively (Table S2; Figures S32 and S33). $T_{el,max.}$ likely decreased as melting temperature and crystallinity decreased due to the increase in chain branching caused by 1-hexene incorporation weakening the intramolecular interactions between polymer chains.[58, 73]

Large scale ethylene/H_2/1-hexene polymerization sMAO supported ^{Me_2}SB(Cp^{Me},I*)$ZrCl_2$ (**3_{sMAO}**), ^{Me_2}SB(Cp,I*)$Zr(CH_2Ph)_2$ (**6_{sMAO}**), ^{Me_2}SB(Cp^{Me},I*)$Zr(CH_2Ph)_2$ (**7_{sMAO}**), and ^{Me_2}SB(Cp,I*)$ZrMe_2$ (**8_{sMAO}**) were studied for ethylene/H_2/1-hexene copolymerization in 2 L steel reactors with 1 L hexane, 0.5 mmol TEA, 0.025–0.050 g pre-catalyst, $[Al_{sMAO}]_0/[Zr]_0$ = 200, and 8 bar ethylene at 80 °C for 1 hour with 0.86% (0.07 bar) H_2 and 10 mL 1-hexene (1% of the total reaction volume). On the addition of 1-hexene to the ethylene/H_2 system, all catalysts except **7_{sMAO}** experienced an initial increase in ethylene uptake rate and an increase in polymerization activity due to the comonomer effect; activities of 8900 and 12000 $kg_{PE}\,mol_{Zr}^{-1}\,h^{-1}\,bar^{-1}$ for **8_{sMAO}** with 0 and 10 mL 1-hexene respectively (Table 4; Figures S24 and S25). This is similar to the positive comonomer effect observed for solution-phase ethylene/1-hexene copolymerization using *rac*-EBIZrCl$_2$ where activity increased by 30% from 12800 to 17200 $kg_{PE}\,mol_{Zr}^{-1}\,h^{-1}\,bar^{-1}$ with 0.5 mol L−1 1-hexene (1.6 bar ethylene and 60 °C).[74] Similar increases in activity on the addition of 1- hexene have also been observed for some Ziegler-Natta-type and Phillips-type polymerization catalysts: $TiCl_4/MgCl_2$ and $TiCl_4/AlCl_3/MgCl_2$ catalysts experienced activities 2.2 and 2.7 times greater respectively on the addition of 0.2 mol L^{-1} 1-hexene (1 bar ethylene and 0.2 bar H_2 at 60 °C),[75] and Cr(VI)/silica–titania and Cr(II)/silica–titania catalysts experienced activities 1.2 and 2.5 times greater respectively on the addition of 0.014 mol L^{-1} 1-hexene (38 bar ethylene at 103 and 97 °C respectively).[62]

Addition of 1-hexene to the ethylene/H_2 system appeared to have no effect on the polymer molecular weights (M_n of approximately 5 kg mol^{-1} for all solid catalysts with 0 and 10 mL 1-hexene), leading PE-wax formation (Table 4; Figures S30 and S31). M_w/M_n was relatively narrow for ethylene/H_2/1-hexene copolymerization (M_w/M_n <4.1), indicating controlled polymerization (Table 4).

Table 4. Slurry-phase ethylene/H_2/1-hexene copolymerization using sMAO supported complexes in a 2 L batch reactor.[a]

Catalyst	1-Hexene [b]	Activity [c]	M_n [d]	M_w/M_n
3$_{\mathbf{sMAO}}$	0	7600	5.0	3.8
	10	12000	4.9	3.2
6$_{\mathbf{sMAO}}$	0	6700	5.2	2.7
	10	11000	4.6	2.8
7$_{\mathbf{sMAO}}$	0	7200	4.6	4.1
	10	2600	5.3	3.7
8$_{\mathbf{sMAO}}$	0	8900	4.8	3.2
	10	12000	4.5	2.8

(a) Polymerization conditions: 0.86% H_2, $[Al_{sMAO}]_0/[Zr]_0 = 200$, TEA (0.5 mmol), ethylene (8 bar), pre-catalyst (0.025–0.050 g), hexane (1 L), 80 °C, and 1 hour; (b) mL; (c) $kg_{PE}\ mol_{Zr}^{-1}\ h^{-1}\ bar^{-1}$, reported to 2 significant figures; (d) kg mol^{-1}, reported to 2 significant figures.

Solid catalysts **7**$_{\mathbf{sMAO}}$ and **8**$_{\mathbf{sMAO}}$ produced polymers with 0.3 and 0.2 mol% 1-hexene incorporation respectively. The polymers produced using **7**$_{\mathbf{sMAO}}$ and **8**$_{\mathbf{sMAO}}$ showed a 7% decrease in polymer crystallinity

(76 and 80% respectively) and a 1 °C decrease in T_m (129 °C for both catalysts) compared to ethylene/H_2 homopolymerization, likely due to an increased amount of chain branching. CEF showed that $T_{el,max.}$ of the copolymers produced using **7_{sMAO}** and **8_{sMAO}** were similar; 98.4 and 98.7 °C respectively (Figure S34).

As postulated, the density of the polymers produced using **7_{sMAO}** for ethylene/H_2/1-hexene copolymerization decreased by 3% compared to ethylene/H_2 polymerization (density of 0.95 and 0.98 g cm^{-3} respectively), likely due to increases in chain branching.

CONCLUSIONS

Nine solid polymethylaluminoxane supported permethylindenyl zirconocenes (sMAO-^{Me_2}SB(Cp^R,I*)ZrX_2) have been studied for their capacity to produce polyethylene waxes. Their H_2 response in two ethylene polymerization systems was investigated using high-throughput screening and 2 L batch reactors.

The catalysts showed remarkable resistance to H_2 deactivation with an approximately constant ethylene uptake maintained throughout the polymerization runs (up to one hour). In high-throughput conditions, the presence of H_2 resulted in a significant decrease in polymer molecular weights; M_n of 120 and 6.1 kg mol^{-1} for sMAO-^{Me_2}SB(Cp,I*)$ZrMe_2$ with 0 and 1.6% H_2 respectively.

The lowest molecular weights were obtained using sMAO-^{Me_2}SB(Cp,I*)$ZrCl_2$ in the 2 L batch reactor with 3.50% H_2 (M_n of 1.7 kg mol^{-1}), highlighting the applications of these catalysts for the production of commercially viable polyethylene waxes. The HDPE produced had very uniform 'popcorn' morphologies, narrow molecular weight distributions, and high crystallinities.

The addition of 1-hexene to the ethylene/H_2 system initially lead to an increase in ethylene uptake rate and polymerization activity (from 3400 to 13000 kg_{PE} mol_{Zr}^{-1} h^{-1} bar^{-1} for sMAO-^{Me_2}SB(Cp^{Me},I*)$ZrMe_2$ with 0 and 125 μL 1-hexene in the high-throughput system). In the batch reactor, the addition of 1-hexene led to no change in polymer molecular weights (M_n of 5 kg mol^{-1} for all catalysts with 0 and 10 mL 1-hexene respectively) and produced polymers with low 1-hexene incorporation (<0.3 mol%).

The key challenge when using metallocene polymerization catalysts to produce PE-waxes is to balance the desired decrease in polymer molecular weights observed in the presence of H_2 with the undesired reduction in polymerization activity that can also occur. Although these catalysts experienced a decrease in polymerization activity when H_2 was introduced to the system, the very low molecular weights of the polymers produced, coupled with the high stability of the catalysts the presence of H_2, makes them ideal candidates to produce polyethylene metallocene waxes on an industrial scale. In addition, the decrease in density in the presence of 1-hexene, coupled with the formation of PE-waxes, offers the possibility of a wide range of applications.

EXPERIMENTAL

High-throughput screening Polymerization experiments were conducted by Dr. Alessio Mingione at HTExplore (University of Naples, Italy) in a Freeslate Parallel Pressure Reactor (PPR) platform consisting of 48 reaction cells contained within a triple MBraun LabMaster Glovebox. The cells (geometric volume ~23 mL, working volume 5 mL) were individually controlled with monitoring of temperature and pressure. Slurry-phase polymerizations were run in semi-continuous mode. Two Vortex stir plates fitted with 6 × 8 racks held the catalyst system components (pre-catalyst and scavenger). The injection system consisted of a dual-arm robot with specialized needles and injectors. Liquid solvents, diluents, and monomers were fed through syringe pumps, with gaseous monomers and diluents fed through direct lines with solenoid valves to individual cells.34 Heptane solvent (5 mL) and TiBA scavenger (10 µmmol) were added to the PPR via robotic syringes, which were then heated to 80 °C and pressurized to 8.3 bar with ethylene. When required, H_2 was added to the reaction vessel via a 0.8 or 1.6% mixed H_2/N_2 feed. Pre-catalyst (0.05–0.15 mg in heptane slurry) and 1-hexene (when required) were injected with robotic syringes and chased by a certain amount of heptane solvent. The reactions were run for 1 hour or until a certain ethylene uptake was reached (8.3 bar for ethylene homopolymerization and 5.5 bar for ethylene/H_2/1-hexene copolymerization), following which the reaction was quenched with an excess of dry air. The polymer samples were transferred to a Genevac EZ-Plus centrifugal evaporator to remove volatiles and then dried under vacuum overnight.

Large scale batch polymerization Polymerizations were performed by Mr. Thawesak Parawan, Mr. Somjet Songnoey, or Mr. Pongsiri Kaeoyok at SCG Chemicals Co., Ltd. (Rayong, Thailand). A 2.5 L steel reactor was charged with hexane (850 mL) and TEA scavenger (0.5 mmol L^{-1}) and saturated with ethylene gas (2 bar). 1-hexene, when required, was added at an overpressure. The reactor was heated to temperature and a mixture of pre-catalyst (0.025–0.050 g) in hexane (20 mL) was added and washed in with a further 130 mL hexane. The ethylene pressure was set to 8 bar and the polymerizations run for 1 hour. On completion, the polymer was decanted and dried in an oven overnight.

ASSOCIATED CONTENT

Supporting Information. The Supporting Information contains general experimental details and additional polymerization data as described by Figures S1–S34 and Tables S1–S2 in the text. This material is available free of charge via the Internet at http://pubs.acs.org.

AUTHOR INFORMATION

Corresponding Author

*E mail: dermot.ohare@chem.ox.ac.uk

Notes

The authors declare no competing financial interest.

ACKNOWLEDGMENT

J. V. L., J.-C. B. and Z. R. T. (SCG Research Fellowship) would like to thank SCG Chemicals Co., Ltd. (Thailand) for financial support; Prof. Vincenzo Busico for the use of HTExplore (University of Naples), Prof. Roberta Cipullo and Dr. Alessio Mingione for running the high-throughput polymerization experiments and polymer analyses (HTExplore); SCG Chemicals Co., Ltd. (Rayong, Thailand) for use of the 2 L batch reactors and Mr. Thawesak Parawan, Mr. Somjet Songnoey, and Mr. Pongsiri Kaeoyok (SCG Chemicals Co., Ltd.) for running batch polymerization experiments and polymer analyses.

REFERENCES

1. Klosin, J.; Fontaine, P. P.; Figueroa, R., Development of group IV molecular catalysts for high temperature ethylene-α-olefin copolymerization reactions. *Acc. Chem. Res.* **2015,** *48* (7), 2004-2016.
2. Hamielec, A. E.; Soares, J. B. P., Polymerization reaction engineering - metallocene catalysts. *Prog. Polym. Sci.* **1996,** *21* (4), 651-706.
3. Kaminsky, W., Zirconocene catalysts for olefin polymerization. *Catal. Today* **1994,** *20* (2), 257-271.
4. Soares, J. B. P.; Hamielec, A. E., Effect of hydrogen and of catalyst prepolymerization with propylene on the polymerization kinetics of ethylene with a non-supported heterogeneous Ziegler-Natta catalyst. *Polymer* **1996,** *37* (20), 4599-4605.
5. Kaminsky, W.; Lüker, H., Influence of hydrogen on the polymerization of ethylene with the homogeneous ziegler system bis(cyclopentadienyl)zirconiumdichloride/aluminoxane. *Makromol. Chem. Rapid. Comm.* **1984,** *5* (4), 225-228.
6. Bohm, L. L., The ethylene polymerization with Ziegler catalysts: fifty years after the discovery. *Angew. Chem., Int. Ed.* **2003,** *42* (41), 5010-5030.
7. Resconi, L.; Cavallo, L.; Fait, A.; Piemontesi, F., Selectivity in propene polymerization with metallocene catalysts. *Chem. Rev.* **2000,** *100* (4), 1253-1346.
8. Hlatky, G. G., Heterogeneous single-site catalysts for olefin polymerization. *Chem. Rev.* **2000,** *100* (4), 1347-1376.
9. Kaminsky, W.; Funck, A.; Haehnsen, H., New application for metallocene catalysts in olefin polymerization. *Dalton Trans.* **2009,** (41), 8803-8810.
10. Sedov, I.; Makhaev, V.; Matkovskii, P. E., Single-site catalysts in the industrial production of polyethylene. *Catal. Ind.* **2012,** *4*, 129-140.
11. Lamb, J. V.; Buffet, J.-C.; Turner, Z. R.; O'Hare, D., Group 4 permethylindenyl complexes for slurry-phase polymerisation of ethylene. *Polym. Chem.* **2019,** *10* (11), 1386-1398.
12. Lamb, J. V.; Buffet, J.-C.; Matley, J. E.; Wright, C. M. R.; Turner, Z. R.; O'Hare, D., Group 4 permethylindenyl complexes for the polymerisation of L-, D- and rac-lactide monomers. *Dalton Trans.* **2019,** *48* (7), 2510-2520.
13. Lamb, J.; O'Hare, D.; Buffet, J.-C.; Khamnaen, T.; Charernsuk, M.; Parawan, T.; Charoenchaidet, S. Unsymmetrical metallocene catalysts and uses thereof. WO2017194943A1, 2017.
14. Lamb, J. V.; Abell, J. C.; McLaren, J. E.; Buffet, J.-C.; Turner, Z. R.; O'Hare, D., Slurry-phase ethylene polymerisation using group 4 ansa-bridged permethylindenyl complexes supported on polymethylaluminoxane. *Mol. Catal.* **2020,** *484*, 110735.
15. Lamb, J. V.; Buffet, J.-C.; Turner, Z. R.; O'Hare, D., Ethylene polymerization using zirconocenes supported on pentafluorophenyl-modified solid polymethylaluminoxane. *Macromolecules* **2020,** *53* (3), 929-935.
16. Finlayson, M. F.; Garrison, C. C.; Guerra, R. E.; Guest, M. J.; Kolthammer, B. W. S.; Parikh, D. R.; Ueligger, S. M. Ultra-low molecular weight ethylene polymers WO1997026287A1, 1997.
17. Napoli, M.; De Vita, R.; Immediata, I.; Longo, P.; Guerra, G., Polyethylene waxes by metallocenes. *Polym. Adv. Technol.* **2011,** *22* (4), 458-462.

18. Umare, P. S.; Tiwari, A. J.; Antony, R.; Tembe, G. L.; Trivedi, B., Synthesis of ultra-low-molecular-weight polyethylene wax using a bulky Ti(IV) aryloxide-alkyl aluminum catalytic system. *Appl. Organomet. Chem.* **2007,** *21* (8), 652-660.

19. Krendlinger, E.; Nowicki, H.-D. Use of metallocene waxes in powder paints. US20050176866A1, 2005.

20. El-Nahas, H. H.; Gad, Y. H.; El-Hady, M. A.; Ramadan, A. B., The study of compatibility of polyethylene and polypropylene by using irradiated polyethylene wax. *Radiat. Eff. Defects Solids* **2012,** *167* (5), 367-376.

21. Ciesińska, W.; Liszyńska, B.; Zieliński, J., Selected thermal properties of polyethylene waxes. *J. Therm. Anal. Calorim.* **2016,** *125* (3), 1439-1443.

22. Herrmann, H.-F.; Hohner, G. Method of using polyolefin waxes. US6080902A, 2000.

23. Eguchi, A.; Sakai, H.; Kigami, T.; Suzuki, C.; Aoki, T. Toner for developing electrostatic latent images US5928825, 1999.

24. Leotsakos, G.; Gravatt, W. M.; Smith, C. P.; Kocur, M. A. Wax dispersion formulations, method of producing same, and uses US8853284B2, 2014.

25. Wahle, B.; Waltenberger, P.; Klink, C.; Thomas, F.; Engels, T. Process for the production of storage stable wax dispersions. US5723137A, 1998.

26. Leotsakos, G.; Gravatt, W. M.; Smith, C. P.; A. Kocur, M. Novel wax dispersion formulations, method of producing same, and uses 2283094B1, 2012.

27. Billuart, G.; Bourgeat-Lami, E.; Lansalot, M.; Monteil, V., Free radical emulsion polymerization of ethylene. *Macromolecules* **2014,** *47* (19), 6591-6600.

28. Xu, X.; Zheng, A. N.; Zhou, X. D.; Guan, Y.; Pan, Y. F.; Xiao, H. N., Antimicrobial polyethylene wax emulsion and its application on active paper-based packaging material. *J. Appl. Polym. Sci.* **2015,** *132* (27), 42214.

29. Luker, H. Polyethylene wax, and a process for the preparation thereof US5023388A, 1991.

30. Chang, M. Method for preparing polyethylene wax by gas phase polymerization. US4914253A, 1990.

31. Broach, J. R.; Thorner, J., High-throughput screening for drug discovery. *Nature* **1996,** *384* (6604), 14-16.

32. Boussie, T. R.; Diamond, G. M.; Goh, C.; Hall, K. A.; LaPointe, A. M.; Leclerc, M.; Lund, C.; Murphy, V.; Shoemaker, J. A. W.; Tracht, U.; Turner, H.; Zhang, J.; Uno, T.; Rosen, R. K.; Stevens, J. C., A fully integrated high-throughput screening methodology for the discovery of new polyolefin catalysts: Discovery of a new class of high temperature single-site group (IV) copolymerization catalysts. *J. Am. Chem. Soc.* **2003,** *125* (14), 4306-4317.

33. Busico, V.; Pellecchia, R.; Cutillo, F.; Cipullo, R., High-throughput screening in olefin-polymerization catalysis: from serendipitous discovery towards rational understanding. *Macromol. Rapid Commun.* **2009,** *30* (20), 1697-1708.

34. Busico, V.; Cipullo, R.; Mingione, A.; Rongo, L., Accelerating the research approach to Ziegler–Natta catalysts. *Ind. Eng. Chem. Res.* **2016,** *55* (10), 2686-2695.

35. Meier, M. A. R.; Hoogenboom, R.; Schubert, U. S., Combinatorial methods, automated synthesis and high-throughput screening in polymer research: The evolution continues. *Macromol. Rapid Commun.* **2004,** *25* (1), 21-33.

36. Boussie, T. R.; Diamond, G. M.; Goh, C.; Hall, K. A.; LaPointe, A. M.; Leclerc, M. K.; Murphy, V.; Shoemaker, J. A. W.; Turner, H.; Rosen, R. K.; Stevens, J. C.; Alfano, F.; Busico, V.; Cipullo, R.; Talarico, G., Nonconventional catalysts for isotactic propene

polymerization in solution developed by using high-throughput-screening technologies. *Angew. Chem., Int. Ed.* **2006,** *45* (20), 3278-3283.

37. Jones, D. J.; Gibson, V. C.; Green, S. M.; Maddox, P. J., Discovery of a new family of chromium ethylene polymerisation catalysts using high throughput screening methodology. *Chem. Commun.* **2002,** (10), 1038-1039.

38. Frazier, K. A.; Boone, H.; Vosepka, P. C.; Stevens, J. C. High activity olefin polymerization catalyst and process. 2005.

39. Thorshaug, K.; Stovneng, J. A.; Rytter, E.; Ystenes, M., Termination, isomerization, and propagation reactions during ethene polymerization catalyzed by Cp2Zr-R+ and Cp*Zr-2-R+. An experimental and theoretical investigation. *Macromolecules* **1998,** *31* (21), 7149-7165.

40. Rappe, A. T.; Skiff, W. M.; Casewit, C. J., Modeling metal-catalyzed olefin polymerization. *Chem. Rev.* **2000,** *100* (4), 1435-1456.

41. Quintanilla, E.; di Lena, F.; Chen, P., Chain transfer to aluminium in MAO-activated metallocene-catalyzed polymerization reactions. *Chem. Commun.* **2006,** (41), 4309-4311.

42. Posch, W., 3 - Polyolefins. In *Applied Plastics Engineering Handbook*, Kutz, M., Ed. William Andrew Publishing: Oxford, 2011; pp 23-48.

43. Novstrup, K. A.; Travia, N. E.; Medvedev, G. A.; Stanciu, C.; Switzer, J. M.; Thomson, K. T.; Delgass, W. N.; Abu-Omar, M. M.; Caruthers, J. M., Mechanistic detail revealed via comprehensive kinetic modeling of [rac-C2H4(1-indenyl)2ZrMe2]-catalyzed 1-hexene polymerization. *J. Am. Chem. Soc.* **2010,** *132* (2), 558-566.

44. Christianson, M. D.; Tan, E. H. P.; Landis, C. R., Stopped-flow NMR: Determining the kinetics of [rac-(C2H4(1-indenyl)2)ZrMe][MeB(C6F5)3]-catalyzed polymerization of 1-hexene by direct observation. *J. Am. Chem. Soc.* **2010,** *132* (33), 11461-11463.

45. Al-Humydi, A.; Garrison, J. C.; Mohammed, M.; Youngs, W. J.; Collins, S., Propene polymerization using ansa-metallocenium ions: catalyst deactivation processes during monomer consumption and molecular structures of the products formed. *Polyhedron* **2005,** *24* (11), 1234-1249.

46. Moscato, B. M.; Zhu, B.; Landis, C. R., Mechanistic investigations into the behavior of a labeled zirconocene polymerization catalyst. *Organometallics* **2012,** *31* (5), 2097-2107.

47. Nelsen, D. L.; Anding, B. J.; Sawicki, J. L.; Christianson, M. D.; Arriola, D. J.; Landis, C. R., Chromophore quench-labeling: an approach to quantifying catalyst speciation as demonstrated for (EBI)ZrMe2/B(C6F5)3-catalyzed polymerization of 1-hexene. *ACS Catal.* **2016,** *6* (11), 7398-7408.

48. Song, F. Q.; Cannon, R. D.; Bochmann, M., Zirconocene-catalyzed propene polymerization: a quenched-flow kinetic study. *J. Am. Chem. Soc.* **2003,** *125* (25), 7641-7653.

49. Bochmann, M., The chemistry of catalyst activation: the case of group 4 polymerization catalysts. *Organometallics* **2010,** *29* (21), 4711-4740.

50. Chu, K. J.; Soares, J. B. P.; Penlidis, A., Effect of hydrogen on ethylene polymerization using in-situ supported metallocene catalysts. *Macromol. Chem. and Phys.* **2000,** *201* (5), 552-557.

51. Shamiri, A.; Chakrabarti, M. H.; Jahan, S.; Hussain, M. A.; Kaminsky, W.; Aravind, P. V.; Yehye, W. A., The influence of Ziegler-Natta and metallocene catalysts on polyolefin structure, properties, and processing ability. *Materials* **2014,** *7* (7), 5069-5108.

52. Chandrasekhar, V., *Inorganic and organometallic polymers*. Springer: 2005.

53. Ramos, J.; Cruz, V.; Munoz-Escalona, A.; Martinez-Salazar, J., Ab initio study of hydrogenolysis as a chain transfer mechanism in olefin polymerization catalyzed by metallocenes. *Polymer* **2000,** *41* (16), 6161-6169.

54. Sivalingam, G.; Natarajan, V.; Sarma, K. R.; Parasuveera, U., Solubility of ethylene in the presence of hydrogen in process solvents under polymerization conditions. *Ind. Eng. Chem. Res.* **2008,** *47* (22), 8940-8946.

55. Kaminsky, W.; Piel, C., Tailoring polyolefins by metallocene catalysis: Kinetic and mechanistic aspects. *J. Mol. Catal. A: Chemical* **2004,** *213* (1), 15-19.

56. Piel, C.; Starck, P.; Seppälä, J. V.; Kaminsky, W., Thermal and mechanical analysis of metallocene-catalyzed ethene–α-olefin copolymers: The influence of the length and number of the crystallizing side chains. *J. Polym. Sci. A: Polym. Chem.* **2006,** *44* (5), 1600-1612.

57. Ushakova, T. M.; Starchak, E. E.; Krasheninnikov, V. G.; Samoilenko, A. A.; Ivchenko, P. V.; Nifant'ev, I. E.; Novokshonova, L. A., Ethylene polymerization and ethylene-1-hexene copolymerization over immobilized metallocene catalysts. *Kinet. Catal.* **2012,** *53* (1), 75-83.

58. Marques, M. D. F. V.; Tiosso, R. B., Comparison of ethylene/1-hexene copolymerization performance using metallocene catalysts supported on both silica and Brazilian mineral clay. *J. Mater. Sci. Eng. Adv. Tech.* **2011,** *4* (2), 149-173.

59. Awudza, J. A. M.; Tait, P. J. T., The "comonomer effect" in ethylene/α-olefin copolymerization using homogeneous and silica-supported Cp2ZrCl2/MAO catalyst systems: Some insights from the kinetics of polymerization, active center studies, and polymerization temperature. *J. Polym. Sci. A: Polym. Chem.* **2008,** *46* (1), 267-277.

60. Novak, A.; Bobak, M.; Kosek, J.; Banaszak, B. J.; Lo, D.; Widya, T.; Ray, W. H.; de Pablo, J. J., Ethylene and 1-hexene sorption in LLDPE under typical gas-phase reactor conditions: experiments. *J. Appl. Polym. Sci.* **2006,** *100* (2), 1124-1136.

61. Banasazak, B. J.; Lo, D.; Widya, T.; Ray, W. H.; de Pablo, J. J.; Novak, A.; Kosek, J., Ethylene and 1-hexene sorption in LLDPE under typical gas phase reactor conditions: a priori simulation and modeling for prediction of experimental observations. *Macromolecules* **2004,** *37* (24), 9139-9150.

62. McDaniel, M. P.; Schwerdtfeger, E. D.; Jensen, M. D., The “comonomer effect” on chromium polymerization catalysts. *J. Catal.* **2014,** *314*, 109-116.

63. Chien, J. C. W.; Yu, Z.; Marques, M. M.; Flores, J. C.; Rausch, M. D., Polymerizations of olefins and diolefins catalyzed by monocyclopentadienyltitanium complexes containing a (dimethylamino)ethyl substituent and comparison with ansa-zirconocene systems. *J. Polym. Sci. A: Polym. Chem.* **1998,** *36* (2), 319-328.

64. Ystenes, M., The trigger mechanism for polymerization of α-olefins with Ziegler-Natta catalysts: A new model based on interaction of two monomers at the transition state and monomer activation of the catalytic centers. *J. Catal.* **1991,** *129* (2), 383-401.

65. Yang, Q.; Jensen, M. D.; McDaniel, M. P., Alternative view of long chain branch formation by metallocene catalysts. *Macromolecules* **2010,** *43* (21), 8836-8852.

66. Paredes, B.; van Grieken, R.; Carrero, A.; Suarez, I.; Soares, J. B. P., Ethylene/1-hexene copolymers produced with MAO/(nBuCp)2ZrCl2 supported on SBA-15 materials with different pore sizes. *Macromol. Chem. and Phys.* **2011,** *212* (15), 1590-1599.

67. Kaminsky, W., New polymers by metallocene catalysis. *Macromol. Chem. and Phys.* **1996,** *197* (12), 3907-3945.

68. Chien, J. C. W.; Nozaki, T., Ethylene-hexene copolymerization by heterogeneous and homogeneous Ziegler-Natta catalysts and the "comonomer" effect. *J. Polym. Sci. A: Polym. Chem.* **1993,** *31* (1), 227-237.

69. Fink, G.; Mülhaupt, R.; Brintzinger, H. H., *Ziegler Catalysts: Recent Scientific Innovations and Technological Improvements*. Springer Berlin Heidelberg: 2012.

70. Jian-ding, Y.; Zhi-qiang, F.; Wei, W., Strong influences of polymerization temperature on ethylene/1-hexene copolymerization catalyzed by (2-PhInd)2ZrCl2/methyl aluminoxane. *J. Zhejiang Univ. Sci. B* **2005,** *6* (10), 1009-1014.

71. Wang, W.; Fan, Z. Q.; Feng, L. X., Ethylene polymerization and ethylene/1-hexene copolymerization using homogeneous and heterogeneous unbridged bisindenyl zirconocene catalysts. *Eur. Polym. J.* **2005,** *41* (10), 2380-2387.

72. Herfert, N.; Montag, P.; Fink, G., Elementary processes of the Ziegler catalysis, 7. Ethylene, α-olefin and norbornene copolymerization with the stereorigid catalyst systems iPr[FluCp]ZrCl2/MAO and Me2Si[Ind]2ZrCl2/MAO. *Makromol. Chem.* **1993,** *194* (11), 3167-3182.

73. Mark, J. E., *Polymer Data Handbook*. Oxford University Press: 2009.

74. Quijada, R.; Dupont, J.; Miranda, M. S. L.; Scipioni, R. B.; Galland, G. B., Copolymerization of ethylene with 1-hexene and 1-octene: correlation between type of catalyst and comonomer incorporated. *Macromol. Chem. and Phys.* **1995,** *196* (12), 3991-4000.

75. Chen, Y.-p.; Fan, Z.-q., Ethylene/1-hexene copolymerization with TiCl4/MgCl2/AlCl3 catalyst in the presence of hydrogen. *Eur. Polym. J.* **2006,** *42* (10), 2441-2449.